ELSEVIER

Journal of Alloys and Compounds 330–332 (2002) 276–279

Journal of ALLOYS AND COMPOUNDS

www.elsevier.com/locate/jallcom

On the structure of epitaxial YH_x films

A. Remhof[a,*], G. Song[b], D. Labergerie[b], J. Isidorsson[a], A. Schreyer[b], F. Güthoff[c], J. Härtwig[d], H. Zabel[b]

[a]*Faculty of Sciences, Division of Physics and Astronomy, Vrije Universiteit, De Boelelaan 1081, NL-1081 AV Amsterdam, The Netherlands*
[b]*Institut für Experimentalphysik/Festkörperphysik, Ruhr-Universität Bochum, D-44780 Bochum, Germany*
[c]*Forschungszentrum Jülich, Institut für Festkörperforschung, D-52425 Jülich, Germany*
[d]*European Synchrotron Radiation Facility, B.P. 220, F-38043 Grenoble Cedex, France*

Abstract

Hydrogen in thin epitaxial films and superlattices has gained renewed interest because of the hydrogen-induced novel optical and magnetic switching properties that have recently been revealed. In this contribution we report on structural details on the effect of hydrogen in epitaxial Y-films. X-ray diffraction reveals the response of the host metal lattice upon hydrogen loading. The hydrogen ordering within the hydride phases as well as the hydrogen concentration can be measured by neutron diffraction. The macroscopic aspects of the hydride formation like domain nucleation and growth are accessible by in-situ real time X-ray diffraction topography.

Keywords: Metal hydrogen systems; Thin films; Phase transitions; X-ray diffraction; Neutron diffraction; X-ray diffraction topography

1. Introduction

Hydrogen in metals has been investigated since Graham discovered in 1866 that palladium can absorb large amounts of hydrogen gas [1–3]. Advances in thin film deposition techniques and hydrogen loading capabilities triggered the research of thin film and multilayered metal hydrogen systems. Exciting new structural and functional properties have been discovered in the recent years, stimulating further work. Among those are the hydrogen tuneable exchange coupling in Fe/Nb [4] and Fe/V [5] superlattices, and an extraordinary adhesion of Nb on Al_2O_3 [6] as probed by the hydrogen induced lattice expansion.

Especially the hydrogen switchable mirror effect in LaH_x and YH_x films fueled the interest in rare earth–hydrogen systems [7]. Depending on the hydrogen concentration different structural phases occur [8]. Pure yttrium forms a hexagonal closed packed crystal which can accommodate hydrogen atoms on interstitial sites up to a critical concentration of $x=H/Y=0.2$. At this value the lattice gas phase (α phase) saturates and the dihydride phase (β phase) starts to precipitate upon further hydrogen loading. It possesses the CaF_2 crystal structure in which yttrium forms the face centered cubic structure, while the hydrogen atoms occupy interstitial places with tetragonal symmetry [9]. Increasing the hydrogen concentration even further, the system saturates in the trihydride phase (γ phase) in this phase the crystallographic structure regains its initial hexagonal symmetry [10]. The structural changes are accompanied by changes in the electronic configuration. While the α and the β phases are shiny metallic, the γ phase is a transparent insulator with an optical bandgap of 1.8 eV. Within thin films the electronic and optical transition is fully reversible [7]. The dynamics of the system, especially the hydrogen diffusion could be visualized in exploiting the optical aspect of the β–γ transition [11]. This contribution focuses on the structural aspects.

2. The microscopic scale

2.1. The response of the yttrium lattice

X-ray diffraction reveals that yttrium evaporated on Nb/Al_2O_3 [12], CaF_2 [13] or W [14] substrates crystallize in the hexagonal $P6_3mmc$ structure with lattice constants of $a=3.36$ Å and $c=5.75$ Å. The symmetry and the interatomic distances are in good agreement with bulk values. Only slight deviations have been observed which

*Corresponding author. Tel.: +31-204-447-926.
E-mail address: aremhof@nat.vu.nl (A. Remhof).

0925-8388/02/$ – see front matter
PII: S0925-8388(01)01442-6

can be attributed to lattice mismatch and/or to initial hydrogen contamination. Longitudinal scans through the out-of plane Y(0002) Bragg reflection exhibit finite size oscillations, proving the high crystalline quality of the films. The observed coherence length agrees with the film thickness as measured by small angle X-ray reflectivity. Transverse scans often show a two component line shape with a resolution limited sharp component superimposed on a broad component. Two component line shapes have been observed in other heteroepitaxial systems as well [15]. The sharp component reflects a long range orientational order of the film induced by the substrate, while the broad component originates from short range order fluctuations of individual domains.

The in-plane epitaxial relation between the Y(0001) film and the Nb(110) buffer layer have been determined by grazing incident X-ray diffraction. 360° transverse scans prove the six-fold symmetry of the Y film while longitudinal scans reveal the alignment between the Y[$1\bar{2}10$] and the Nb[002] direction.

In-situ hydrogen loading at room temperature up to YH_3 degrades slightly the structural long range order of the Y planes parallel to the surface, causing the narrow component of the rocking curve to vanish and the broad component to broaden. The longitudinal width of the Bragg peak stays constant, showing a constant coherence length even in the fully hydrogenated state. Following the out-of plane Y(0002) Bragg peak in longitudinal scans show discrete and abrupt changes of the lattice parameter, indicating structural changes to the dihydride (YH_2) and to the trihydride (YH_3) phase. Between the YH_2 and the YH_3 phase no further loss in structural coherence is observed and the transition is fully reversible. The temporal development of a slow loading experiment at a hydrogen pressure of 20 mbar at room temperature is shown in Fig. 1.

The symmetry and the epitaxial relation are maintained during hydrogen uptake. The lattice expansion is highly anisotropic and effects mostly the *c*-axis. Nevertheless, the 0.5% in-plane expansion is surprisingly isotropic, regardless of the simultaneously 3.8% expanding Nb buffer layer.

Neither the scans along the (000*l*) rod nor the in-plane measurements are sensitive to the changing stacking sequence of the hexagonal basal planes during the hcp–fcc transition. Only scans along reciprocal lattice rods containing in-plane as well as out-of plane components prove that also in thin films the phase transitions in the H–Y system comprise a rearrangement of the stacking sequence within the Y lattice.

This study agrees with X-ray photoelectron diffraction measurements on yttrium films grown on tungsten single crystals [14]. In combination with the 10% lattice expansion, the complete reversibility of the YH_2–YH_3 transition is a remarkable observation.

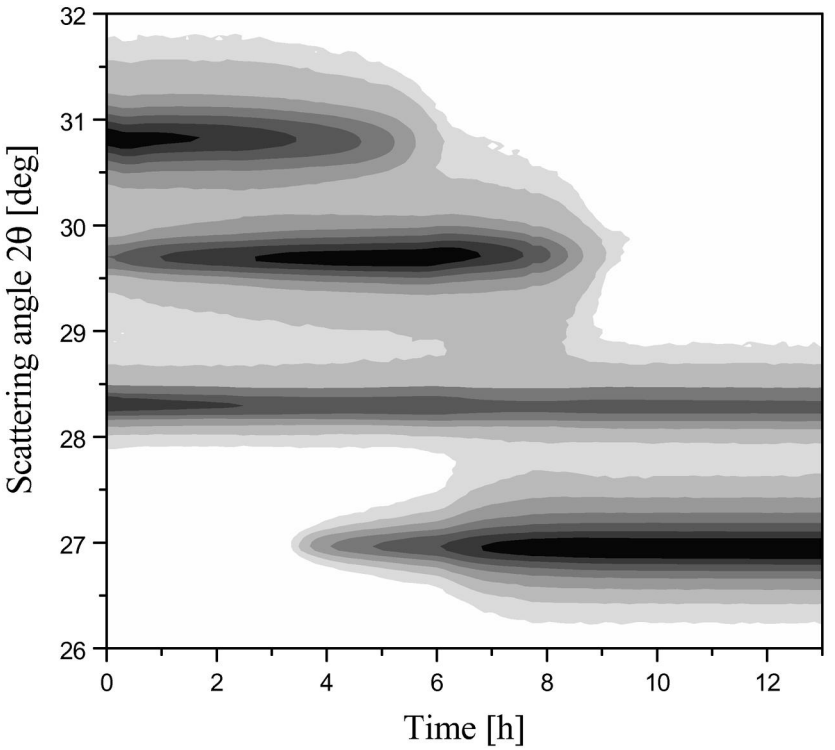

Fig. 1. Sequence of longitudinal X-ray scans (Cu Kα radiation) of a gas phase hydrogen loading at 20 mbar of a Pd capped Y layer grown on CaF_2. From top to bottom the peaks from the α and β and γ phase appear. The constant reflection at 28.28° originates from the substrate.

2.2. Hydrogen ordering and isotope exchange

Due to the large neutron scattering cross section, hydrogen and deuterium can easily be detected by neutron diffraction, in contrast to X-ray scattering. Furthermore, neutron diffraction distinguishes between the different hydrogen isotopes via their different sign of the neutron scattering length. At small momentum transfer, i.e. in small angle neutron reflectivity measurements the angle of total external reflection depends sensitively on the hydrogen concentration and on the isotope by probing the average scattering length density of the sample. Hydrogen resolved as a lattice gas in the Y-film leads to a decrease of the critical angle, as it has a negative neutron scattering length. In the hydride phases (YH_2 and YH_3) phase the average scattering length density becomes negative and no total reflection occurs. In other words, even at very low angles all neutrons penetrate the sample.

Deuterium has the opposite effect. The edge of total reflection shifts to higher angles as deuterium enters the sample. The shift of the critical angle stops when the Y film reaches saturation in the YD_3 phase. A further increase of the surrounding deuterium pressure then has no additional effect on the angular position of the critical angle.

The different neutron scattering lengths of the two hydrogen isotopes also influence the structure factor of the Bragg reflections in high angle neutron diffraction. The intensity ratio of the YH_3 (0002) and the YD_3 (0002) reacts very sensitively on the respective H (D) concentration. Neutron scattering therefore provides two independent ways to measure the amount of hydrogen (deuterium) within the Y film. From both methods a slightly substoichiometric trihydride phase is determined.

With neutron scattering and using different isotopes also the stability of the hydrides can be tested. By exchanging the hydrogen isotope in the surrounding atmosphere of the sample, the edge of total reflection as well as the intensity of the specular Bragg reflection can switched reversibly between the respective values of YH_3 and YD_3. Thus measurements on hydrogenated and deuterated films show the complete replacability of H by D and vice versa.

Furthermore neutron diffraction also reveals the positional order of the hydrogen atoms within the host lattice. In the YD_3 structure, neutron scattering experiments show additional Bragg reflections, which are not visible in X-ray diffraction. They stem from the sinusoidal deuterium ordering within the basal plane. All structural measurements carried out so far are in agreement with the proposed *($P\bar{3}c1$)* structure [12], but some doubts still remain [16].

3. The macroscopic scale

For technical applications, the macroscopic structure and the kinetics of the yttrium hydrides are of interest. Therefore an imaging technique is required to visualize the structural changes during hydrogen loading and unloading. X-ray diffraction topography turned out to be a suitable tool for those studies [17]. This non-destructive method probes the whole volume of the sample under investigation. Based on Bragg diffraction it exploits local variations of the sample reflecting power. Thus it visualizes inhomogeneities such as defects, domains or phases within the crystal under investigation. By using parallel and monochromatic radiation, a connection between a point of the two-dimensional image on the position-sensitive detector e.g. a photographic film and a small volume element within the sample is established. In a heteroepitaxial system (like Y on Nb/Al_2O_3) all lattice planes are parallel but different films exhibit different lattice spacings. Hydrogen loading alters the lattice parameters of the Y film, but it maintains the parallelity of the crystallographic planes in the growth direction. Rotating the sample about an axis normal to the scattering plane, the reflections of the different layers (or regions of different phases) will be spatially separated on the photographic film. This lattice parameter contrast can be used to distinguish between the Y layer and the substrate and to visualize the response of the metal lattices to the hydrogenation.

The small scattering volume of thin films and the requirement to have a spatially extended, monochromatic beam, a small divergence and a high photon flux requires synchrotron radiation.

Fig. 2 depicts a series of topographic images during the

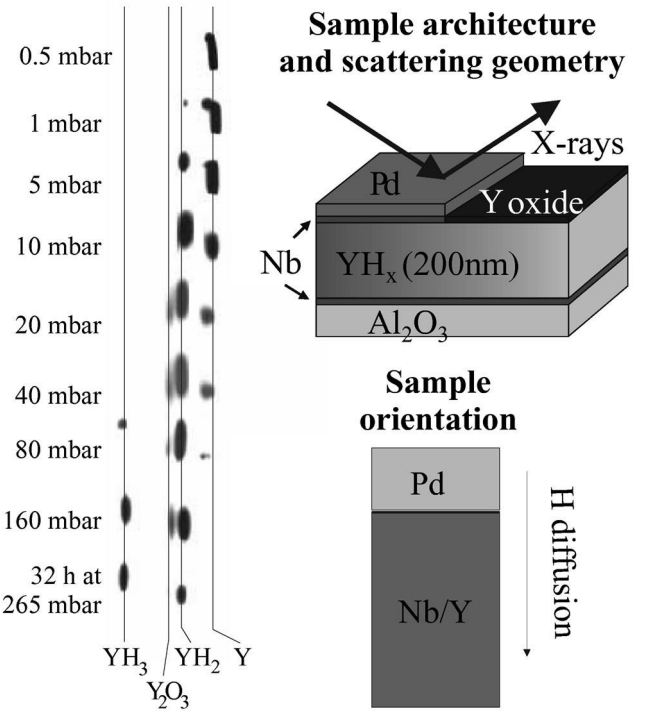

Fig. 2. Series of X-ray diffraction topographies of the first hydrogenation (right). The inset on the left side (top) shows the side view of the partially Pd covered sample together with the scattering geometry, while the inset at the bottom depicts the sample orientation during the exposures.

first loading. All images were taken at 300°C. To visualize lateral hydrogen diffusion, a small Pd stripe evaporated on top of the Y film serves as a hydrogen window. While the hydrogen gas may enter the sample via the Pd stripe, the rest of the sample covered with the natural yttrium oxide is impervious to hydrogen.

A series of X-ray diffraction topographies of a partially Pd caped is shown in Fig. 2. Each picture in Fig. 2 depicts a 7-mm long part of the sample.

The extent of each recorded topograph corresponds directly to the extent of the respective phase within the sample. Geometrical effects compress the image of the 10-mm wide sample to about 1 mm on the photographic film. Hydrogenation of the sample progresses from top to bottom with increasing pressure. First, the lattice expansion in the α-phase, followed by the nucleation of the β-phase can be observed in the Pd covered part of the sample. Afterwards lateral hydrogen diffusion starts, accompanied by the structural phase transitions as described in the introduction. The precipitation of YH_2 starts simultaneously at arbitrary places in the Pd-covered part of the sample. The homogeneously distributed YH_2 domains could not be spatially resolved. Therefore their size can only be estimated to be smaller than 1 μm (film resolution). As soon as the Pd covered part of the sample is fully loaded to the β-phase, lateral diffusion starts. There is no sharp diffusion front visible in the Y film. A region of coexisting α and β phases can still be observed. Obviously the hydrogen finds diffusion paths in the film where it can advance faster in one region than in others, leaving domains of lower hydrogen concentration behind.

The γ phase starts to nucleate at a pressure of 80 mbar. Like the occurrence of the β phase at 1 mbar, both phases coexist beneath the Pd cap layer before the hydrogen-rich phase starts to diffuse along the sample at higher pressures. During the diffusion process, the phase border of the YH_3 behaves similar to the YH_2 border. There is no visible change in the domain size. Again a region of phase coexistence propagates in front of the homogeneous YH_3 phase. Hydrogen diffusion within the investigated sample is slow, especially in the YH_3 phase. Even after 36 h in a hydrogen atmosphere of 265 mbar the hydrogen front line of the YH_3 phase just moved 2 mm while the rest of the Y film changed completely to YH_2. Due to the low velocity of the diffusion, thermodynamic equilibrium has not been achieved.

Removing the hydrogen atmosphere completely and keeping the temperature constant at 300°C expels the hydrogen partially from the sample. Desorption of the hydrogen takes place through the Pd cap layer. First the hydrogen becomes expelled from the Pd-covered part. Later on the hydrogen from this middle region diffuses towards the Pd window, where it escapes from the sample, causing the γ phase to vanish gradually.

Hydrogen diffusion can be observed by the lateral progression of the phase boundary. At $p_{H_2} = 800$ mbar and at 300°C, the YH_3 front moves with an effective mobility of 5×10^{-6} cm^2/s.

Acknowledgements

We would like to thank R. Griessen and S.J. van der Molen for fruitful discussions. This work was supported by the Bundesministerium für Bildung und Forschung under Contract Nos. ZA4BC1 and ZA4BC2 and the EU-TMR project Metal-hydride films with switchable physical properties (Project No. ERB FMRX-CT98-187), which we gratefully acknowledge.

References

[1] Y. Fukai, The Metal–Hydrogen System, Springer–Verlag, Berlin, 1993.
[2] G. Alefeld, J. Völkl (Eds.), Hydrogen in Metals, Vols. I and II, Springer-Verlag, Berlin, 1978.
[3] L. Schlapbach (Ed.), Hydrogen in Intermetallic Compounds, Vols. I and II, Springer-Verlag, Berlin, 1988.
[4] F. Klose, Ch. Rehm, D. Nagengast, H. Maletta, A. Weidinger, Phys. Rev. Lett. 78 (1997) 1150.
[5] B. Hjörvarsson, J.A. Anderson, P. Isberg, T. Watanabe, T.J. Udovic, G. Anderson, C.F. Majkrzak, Phys. Rev. Lett. 79 (1997) 901.
[6] G. Song, A. Remhof, K. Theiss-Bröhl, H. Zabel, Phys. Rev. Lett. 79 (1997) 5062.
[7] J.N. Huiberts, R. Griessen, J.H. Rector, R.J. Wijngarten, J.P. Dekker, D.G. de Groot, N.J. Koeman, Nature (London) 380 (1996) 231.
[8] P. Vadja, in: K.A. Gschneidner, L. Eyring (Eds.), Handbook On the Physics and Chemistry of Rare Earth, Edited By, Vol. 20, Elsevier, Amsterdam, 1995.
[9] R.W.G. Wyckoff, Crystal Structures, Vol. 1, Interscience, New York, 1966.
[10] T.J. Udovic, Q. Huang, J.J. Rush, J. Phys. Chem. Solids 57 (1996) 423.
[11] F.J.A. den Broeder, S.J. van der Molen, M. Kremers, J.N. Huiberts, D.G. Nagengast, A.T.M. van Gogh, W.S. Huisman, N.J. Koeman, B. Dam, J.H. Rector, S. Plota, M. Haaksma, R.M.N. Hanzen, R.M. Jungblut, P.A. Duine, R. Griessen, Nature (London) 394 (1998) 656.
[12] A. Remhof, G. Song, C. Sutter, A. Schreyer, R. Siebrecht, H. Zabel, F. Güthoff, J. Windgasse, Phys. Rev. B 59 (1999) 6689.
[13] D.G. Nagengast, J.W.J. Kerssemakers, A.T.M. van Gogh, B. Dam, R. Griessen, Appl. Phys. Lett. 75 (1999) 1743.
[14] J. Hayoz, S. Sarbach, Th. Pillo, E. Boschung, D. Naumovic, P. Aebi, L. Schlapbach, Phys. Rev. B 58 (1998) R4270.
[15] B. Wölfing, K. Theis-Böhl, C. Sutter, H. Zabel, J. Phys. Condens. Matter. 11 (1999) 2669–2678.
[16] T.J. Udovic, Q. Huang, R.W. Erwin, B. Hjörvarsson, R.C.C. Ward, Phys. Rev. B 61 (2000) 12701.
[17] A. Remhof, G. Song, C. Sutter, D. Labergerie, M. Hübener, H. Zabel, J. Härtwig, Phys. Rev. B 62 (2000) 2164.